International Journal of Mass Spectrometry 313 (2012) 41–46

Contents lists available at SciVerse ScienceDirect

International Journal of Mass Spectrometry

journal homepage: www.elsevier.com/locate/ijms

Electron loss accompanied by target ionization for He^+ and Li^{2+} on H and He in low- to intermediate-energy regime

Baowei Ding*, Hongchao Li, Weijie Zhang

Institute of Nuclear Physics, Lanzhou University, Lanzhou 730000, People's Republic of China

ARTICLE INFO

Article history:
Received 19 July 2011
Received in revised form
26 December 2011
Accepted 26 December 2011
Available online 10 January 2012

PACS:
34.70.+e
34.50.Fa

Keywords:
Electron loss
Ionization
Ion-atom collision

ABSTRACT

The cross sections for single electron loss (SL), single electron loss associated with single ionization (SLSI) and single electron loss associated with double ionization (SLDI) in collisions of one-electron ions He^+, Li^{2+} with atomic hydrogen and helium in low- to intermediate-energy regime are calculated by considering the distribution of both target and projectile electrons. The calculated results are compared with the available experimental data. Good agreements are obtained.

1. Introduction

Collisions between partially stripped ions and target atoms may result in ionization of projectiles. This process is usually called 'electron loss'. During the last several decades, charge-changing collisions involving the electron-loss process have been of interest due to their importance to such diverse fields as accelerator technology [1], astrophysics [2], plasma physics [3] and construction of large storage rings [4]. In the low- to intermediate-energy regime, the simultaneous ionization of both collision partners occurs in a certain probability. For this reason, these collision processes are more complex than bare-projectile-neutral-atom collisions. The electron-loss process for one-electron ions is a simple collision system and of great interest since it plays a critical role on establishing or testing theories which enable us to predict mechanisms of more complex partners. On the other hand, the complexity grows up in the treatment of electron loss for the complicated target due to the nonlinear increase in the possible ways to reach a given target final charge state. In low to intermediate energies, experimental measurements of the electron loss from one-electron ions colliding with various targets have been performed by different groups [5–17], but theoretical analysis of such processes is complicated due to the fact that electron loss, capture and ionization are comparable to some extent and also strongly couple each other.

As far as the classical treatments in dealing with the ion-atom-collision process, the Bohr–Lindhard (B–L) model [18], in which two critical distances (the release radius R_R and capture radius R_C) are proposed, has to be one of the most famous theories. It suggests that the target electron can be released when the projectile is close enough so that its Coulomb force is equal to the binding force of the electron in the atom. That is $q/R_R^2 = v_e^2/a$, where q is the charge state of the projectile, v_e and a is the target-electron velocity and its orbital radius, respectively. The release distance is then given by $R_R = (qa)^{1/2}/v_e$. When the potential energy of this released electron in the projectile frame is larger than its kinetic energy, the capture then occurs possibly. The capture distance R_C is determined by $R_C = 2q/v_P^2$ in which v_P is the projectile velocity. If $R_C > R_R$, the capture cross section σ_C is given by $\sigma_C = \pi R_R^2$, which means one released electron will be absolutely captured by the projectile. In this case, the capture cross section is independent of the impact velocity. However, because $R_C < R_R$ for higher energies, both ionization and capture are possible for a released electron. Supposed that the release is a gradual process, it takes place with a probability per unit time of the order of v_e/a. Within R_C, the release probability is in the order of $(R_C/v_P)(v_e/a)$. In this case, the capture cross section is obtained as $\sigma_C = 8\pi q^3 \cdot (v_e/a) \cdot v_P^{-7}$. Thus, the B–L model predicts the capture cross section at higher velocities decreases as v_P^{-7}. While ionization occurs when the energy transferred exceeds

* Corresponding author.
E-mail addresses: dingbw@lzu.edu.cn, dingbw2002@yahoo.com.cn (B. Ding).

1387-3806/$ – see front matter © 2011 Elsevier B.V. All rights reserved.
doi:10.1016/j.ijms.2011.12.016

the ionization potential. Therefore, the ionization cross section σ_I is obtained by the integration of the Rutherford cross section from the ionization potential I to the maximum transferable energy $2v_P^2$, $\sigma_I = 4\pi q^2 \cdot v_P^{-2} \cdot [(2I)^{-1} - (2v_P)^{-2}]$. Following Bohr and Lindhard, Brandt [19] and Ben-Itzhak et al. [20] calculated the capture cross sections in fast collisions using the impact-parameter dependences by taking into account the different times spent by projectiles with different impact parameters, respectively. Based on their works, the multiple ionization cross sections in collisions of various charge-state ions with H and He targets have been evaluated in a wide energy range in our previous papers [21–24]. The reasonable results were obtained.

This method is extended in the present article, which reports on calculations of total cross sections for single electron loss and cross sections for single electron loss accompanied by ionization for one-electron projectiles (He^+ and Li^{2+}) in collisions with atomic hydrogen and helium in low- to intermediate-energy regime. The processes investigated here can be described as

$$X^{(Z-1)+}(Z_P) + A(Z_T) \rightarrow X^{Z+}(Z_P) + A^{m+}(Z_T) + (m+1)e^- \quad (0 \le m \le Z_T), \tag{1}$$

in which $X^{Z+}(Z_P)$ and $A(Z_T)$ are one-electron projectile (where Z_P is the charge of its nucleus) and the target atom with nuclear charge Z_T, respectively. $\sigma^{0m}_{Z_P-1,Z_P}$, in which the subscripts are the initial and final states of the projectile and the superscripts are the initial and final states of the target atom, is used to denote the cross section of single electron loss accompanied by m-fold ionization of the target atom. $m = 1, 2$ represent single electron loss associated with single ionization (SLSI) and double ionization (SLDI), respectively. Then the total single electron loss (SL) cross section is

$$\sigma_{Z_P-1,Z_P} = \sum_m \sigma^{0m}_{Z_P-1,Z_P} \tag{2}$$

The present obtained results are compared with the available experimental data, and in general, good agreement is obtained. Throughout this paper, atomic units ($e = m = \hbar = 1$) are used unless otherwise stated.

2. Method

We assume that a target atom is static in the origin of the coordinates and a projectile moves with a constant velocity along a linear trajectory. The coordinate of the projectile nucleus is given by $\mathbf{S} = \mathbf{v_P}t + \mathbf{b}$, where $\mathbf{b}$ is the impact parameter with respect to the target nucleus. The release and capture conditions that are derived from the B–L model [18] turn into, respectively

$$\frac{q_P}{|\mathbf{S}-\mathbf{r}|^2} = \frac{v_e^2}{|\mathbf{r}|}, \tag{3}$$

and

$$\frac{q_P}{|\mathbf{S}-\mathbf{r}|} = \frac{1}{2}v_P^2, \tag{4}$$

where $\mathbf{r}$ is the coordinate of the target electron. Only when the impact parameter of the projectile with respect to the target electron, ρ, is less than the release distance, $|\mathbf{R_R}| = |\mathbf{S}-\mathbf{r}|$, the release for a target electron is possible. Then release probability $F_R(\rho,q,v_P,r)$ for one electron is given by

$$F_R(\rho, q_P, v_P, r) = \frac{2}{\tau} \cdot \frac{\sqrt{R_R^2 - \rho^2}}{v_P}, \tag{5}$$

with $1/\tau$ being the release rate. Here a simple form of the release rate, $1/\tau \sim v_e$, is employed. The released electron may be captured if it is in the capture sphere. Thus the capture probability is given by

$$F_C(\rho, q_P, v_P, r) = \frac{2}{\tau} \cdot \frac{\sqrt{R^2 - \rho^2}}{v_P}, \tag{6}$$

where R satisfies $R = R_R$ if $R_C > R_R$ and $R = R_C$ otherwise. We suppose that when the projectile approaches the target nuclei, the released electron will move together with the projectile, and only when it moves away from the nuclei, the ionization is classically allowed. Thus the ionization probability $F_I(\rho,q_P,v_P,r)$ is given by

$$F_I(\rho, q_P, v_P, r) = \frac{[F_R(\rho, q_P, v_P, r) - F_C(\rho, q_P, v_P, r)]}{2}, \tag{7}$$

The electron density, $|\psi(\mathbf{r})|^2$, of the target atom is supposed as a simple exponential function of the distance:

$$|\psi(\mathbf{r})|^2 = \frac{Z_T^{*3}}{\pi} \exp(-2Z_T^* r), \tag{8}$$

where Z_T^* is the effective nuclear charge. The probability that the electron is in $d^3\mathbf{r}$ at $\mathbf{r}$ is $|\psi(\mathbf{r})|^2 d^3\mathbf{r}$. Thus release, ionization and capture probabilities are obtained as

$$P_{R,I,C}(b, q_P, v_P) = \int F_{R,I,C}(\rho, q_P, v_P, r)|\psi(\mathbf{r})|^2 d^3\mathbf{r}, \tag{9}$$

It is more convenience to perform this integral in cylinder coordinate. For this purpose, the formula (9) can be rewritten as

$$P_{R,I,C}(b, q_P, v_P) = \frac{Z_T^{*3}}{\pi} \int_0^\infty d\rho\rho \int_0^{2\pi} d\varphi \int_{-\infty}^{+\infty} dz F_{R,I,C} \times \exp(-2Z_T^* \cdot r(b, \rho, \varphi, z)), \tag{10}$$

Since probabilities P_I and P_C may be larger than unity, we use the unitarized formula [25],

$$P_{UI,UC}(b, q_P, v_P) = \frac{P_{I,C}}{P_I + P_C} \cdot [1 - \exp(-(P_I + P_C))], \tag{11}$$

in which the subscript 'U' denotes the corresponding unitarized probability.

In the case of the projectile, the electron density can be given by

$$|\psi_P(r')|^2 = \frac{Z_P^{*3}}{\pi} \exp(-2Z_P^* r'), \tag{12}$$

where Z_P^* is the effective charge of the projectile nucleus ($Z_P^* = Z_P$ for one-electron ions), and $|\mathbf{r}'| = |\mathbf{r_{pe}} - \mathbf{S}|$ is the distance between the projectile electron and nucleus with $\mathbf{r_{pe}}$ is the coordinate of the projectile electron. In order to derive the electron-loss probability, according to the method in Eqs. (3) and (4), the distances for projectile-electron release (R_R') and capture (R_C') can be obtained. Then the release and capture probabilities for the projectile electron are written as

$$F'_R(\rho', q_T, v_P, r') = \frac{2}{\tau'} \cdot \frac{\sqrt{R_R'^2 - \rho'^2}}{v_P}, \tag{13}$$

$$F'_C(\rho', q_T, v_P, r') = \frac{2}{\tau'} \cdot \frac{\sqrt{R'^2 - \rho'^2}}{v_P} \tag{14}$$

here $\tau' = 1/v_e'$ where v_e' is the orbital velocity of the projectile electron, q_T is the effective charge of the target, ρ' is the impact parameter of the target nucleus with respect to the projectile electron, and R' satisfies $R' = R_R'$ if $R_C' > R_R'$ and $R' = R_C'$ otherwise. Then the electron-loss probability is given as

$$F_L(\rho', q_T, v_P, r') = \frac{[F'_R(\rho', q_T, v_P, r') - F_C(\rho', q_T, v_P, r')]}{2} \tag{15}$$

The electron-loss probability $P_L(b,q_T,v_P)$ at a given impact parameter b can be calculated by the integration with the same form in Eq. (10). Correspondingly, the unitarized electron-loss probability $P_{UL}(b,q_T,v_P)$ can be obtained.

It should be noted that the electron loss is often accompanied by the electron capture in a same collision event, resulting in a final charge state equal to the initial one, which is not usually identified in experiments. Therefore, in order to compare calculations with experimental data, we have to remove the component due to the electron loss associated with the electron capture from the total electron-loss cross section. For collisions of one-electron ions $X^{(Z-1)+}$ with the H target, the SL cross section is given as

$$\sigma_{Z_P-1,Z_P} = 2\pi \int_0^\infty P_{UL}(1-P_{UC})bdb, \tag{16}$$

The SLSI cross section can be given as

$$\sigma^{01}_{Z_P-1,Z_P} = 2\pi \int_0^\infty P_{UL}P_{UI}bdb, \tag{17}$$

In the case of the He target by one-electron ions $X^{(Z_P-1)+}$, two electrons are supposed to depart from the target one by one. They have the same ionization potential at the beginning, and then once one of them is removed, the other one will be exposed to a stronger field due to the increasing Coulomb force from the target nucleus. Thus the SL cross section for collisions of one-electron ions $X^{(Z-1)+}$ with He is given as

$$\sigma_{Z_P-1,Z_P} = 2\pi \int_0^\infty P_{UL}(1-P_{UC1})(1-P_{UC2})bdb, \tag{18}$$

where the subscripts 1 and 2 denote the first and second electrons of the helium atom, respectively. Correspondingly, The SLSI cross section can be given by

$$\sigma^{01}_{Z_P-1,Z_P} = 2\pi \int_0^\infty 2P_{UL}P_{UI1}(1-P_{UI2}-P_{UC2})bdb, \tag{19}$$

While the SLDI cross section is given as

$$\sigma^{02}_{Z_P-1,Z_P} = 2\pi \int_0^\infty P_{UL}P_{UI1}P_{UI2}bdb, \tag{20}$$

3. Results and discussion

We have calculated the cross sections for $He^+ + H$, He and $Li^{2+} + H$, He collisions in low- to intermediate-energy regime. The effective charge q_P for the partially stripped ion $X^{(Z_P-1)+}$ should be larger than its charge state (Z_P-1), i.e., $q_P > Z_P - 1$. In present calculations, for the simplicity, we choose $q_P = 1.345$ for He^+ while $q_P = 2$ for Li^{2+}. In addition, the removal of the target electron will increase the target effective charge q_T which exerts on the projectile electron. Because the release probability of the target electron increases as the projectile charge state (Z_P-1) increases, one can see that the higher projectile charge state is, the larger q_T becomes. However, it is difficult to define a q_T formula. For simplicity, here the following form of q_T is applied

$$q_T = Z_T[1-\exp(-S(Z_P-1))], \tag{21}$$

where $S = 1$ for $\sigma_{Z_P-1,ZP}$ and $S = 1.12$ for $\sigma^{0,m}_{Z_P-1,Z_P}(m \neq 0)$. The effective charge in Eq. (8) $Z_T^* = 1$ for H, $Z_T^* = 1.345$ and 2 for the first and second electrons of the He atom, respectively.

Fig. 1 shows the impact-parameter dependences of probabilities for (a) single electron loss, (b) single electron loss associated with single ionization and (c) single electron loss associated with double ionization for various collisions at the impact energy $E = 400$ keV/u. It is obvious that, for a given target and process, the range of effective impact parameter induced by He^+ is larger than that by Li^{2+}, which is due to the stronger bound on the projectile electron by Li^{2+}. However, this is not so clear for single electron loss with double ionization shown in Fig. 1(c), which is because double ionization probability is far smaller than that of single ionization. For the collision by Li^{2+}, the closer distance between the projectile and the target has to be required in order to release the projectile electron. On the other hand, for a given projectile and process, results show the larger impact-parameter range for the He target. This is because the effective charge of He is larger than that of H as discussed in Eq. (21). It can be also seen from Fig. 1 that the effective impact parameter ranges for SL, SLSI and SLDI decrease in the sequence. As described by Eq. (2), in the SL process, the target electron(s) may still stay in the target or be ionized. In other words $m = 0$, 1 for the H target and $m = 0$, 1, 2 for the He target, respectively. However, In the SLSI and SLDI processes, ionization of both collision partners occurs and the outgoing channel for target electron(s) is restricted to $m = 1$ for SLSI and $m = 2$ for SLDI, respectively. It is also noticed in Fig. 1 that, for a given target at $v_p = 4$ a.u., the maximum value is always higher for He^+ projectile than for Li^{2+} in Fig. 1(a) and (b), but opposite behavior in Fig. 1(c). This is reasonable due to the different velocity dependences for various reaction channels.

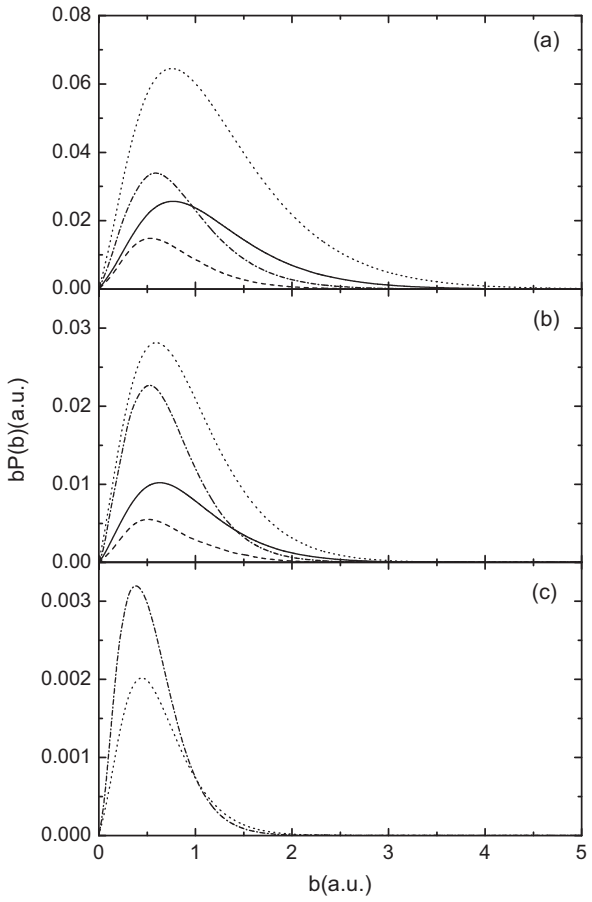

Fig. 1. The impact-parameter dependences of probabilities for electron loss at $v_P = 4$ a.u. (a) Single electron loss. Solid line, $He^+ + H$; dashed line, $Li^{2+} + H$; dotted line, $He^+ + He$; dash-dotted line, $Li^{2+} + He$. (b) Single electron loss with single ionization. Solid line, $He^+ + H$; dashed line, $Li^{2+} + H$; dotted line, $He^+ + He$; dash-dotted line, $Li^{2+} + He$. (c) Single electron loss with double ionization. Dotted line, $He^+ + He$; dash-dotted line, $Li^{2+} + He$.

The calculated cross sections are displayed as functions of the projectile energy in Figs. 2–6 and compared with the available experimental data [6–14] except for the SLSI process for $He^+ + H$ and $Li^{2+} + H$ collisions. It can be seen that the calculated results are in good agreement with experiments. All results show similar trends.

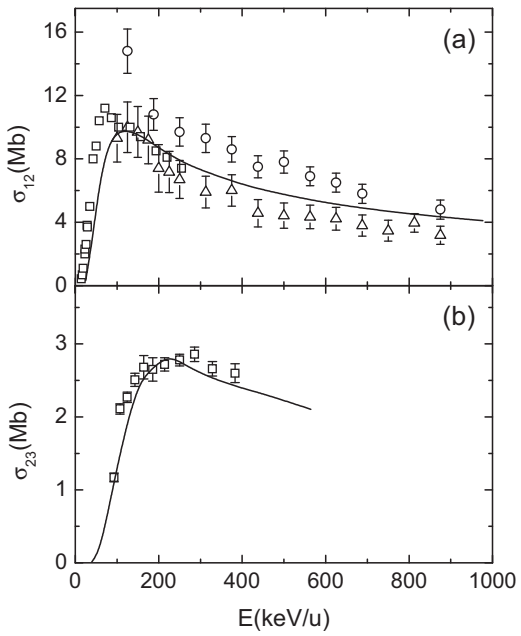

Fig. 2. Electron-loss cross sections (in Mb) in collisions of ions with atomic hydrogen as a function of the projectile energy. Calculation: solid line. (a) $He^+ + H$. Experiment: open squares, Ref. [6]; open circles, Ref. [7]; open triangles, Ref. [8]. (b) $Li^{2+} + H$. Experiment: open squares, Ref. [9].

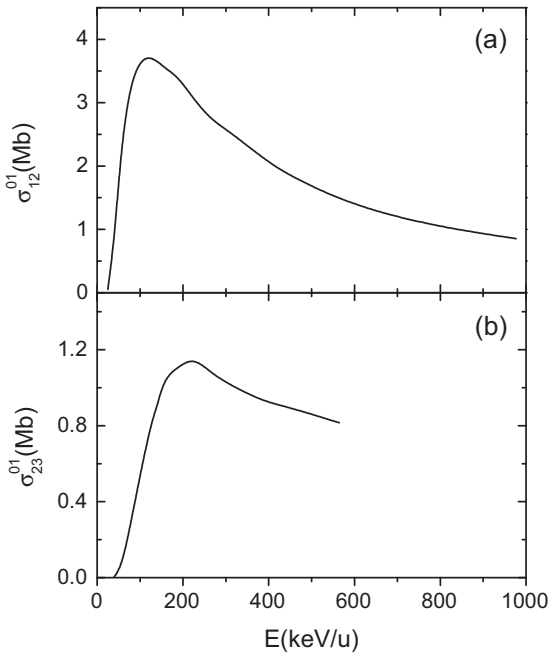

Fig. 4. Cross sections (in Mb) for electron loss accompanied by single ionization in collisions of ions with atomic hydrogen as a function of the projectile energy. Calculation: solid line. (a) $He^+ + H$. (b) $Li^{2+} + H$.

For small ion energies, due to the large capture probability, the cross section is small relatively. Because the capture radius is in proportion to v_P^{-2}, the cross section rises rapidly with the increasing impact energy. The present calculations can give the correct peak position E_{max}. At higher energies than E_{max} the cross section is drastically reduced with the increasing energy. Such shape can be explained in terms of the projectile-target interaction time. Due to the decrease of the interaction time, the effective number of collisions between the target and the projectile is reduced.

As seen from the figures, for the given process and target, E_{max} by Li^{2+} is larger than that by He^+. This feature for single electron loss can be understood according to Eqs. (13)–(15). For the simplicity, the electron-loss probability F_L at $\rho' = 0$ will reach a maximum when

$$\frac{dF_L(\rho'=0)}{dv_P} = \frac{d}{dv_P}\left[\frac{1}{\tau'}\left(\frac{R'_R}{v_P} - \frac{R'_C}{v_P}\right)\right] = 0 \tag{22}$$

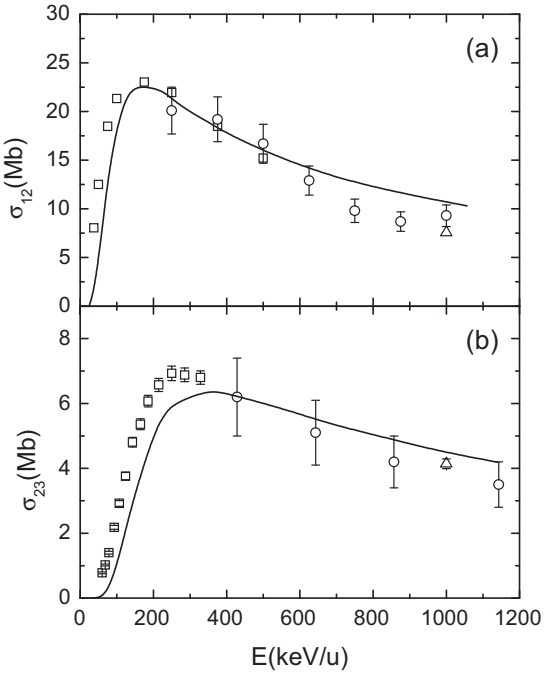

Fig. 3. Electron-loss cross sections (in Mb) in collisions of ions with helium as a function of the projectile energy. Calculation: solid line. (a) $He^+ + He$. Experiment: open squares, Ref. [10]; open circles, Ref. [11]; open triangles, Ref. [12]. (b) $Li^{2+} + He$. Experiment: open squares, Ref. [9]; open circles, Ref. [13]; open triangles, Ref. [12].

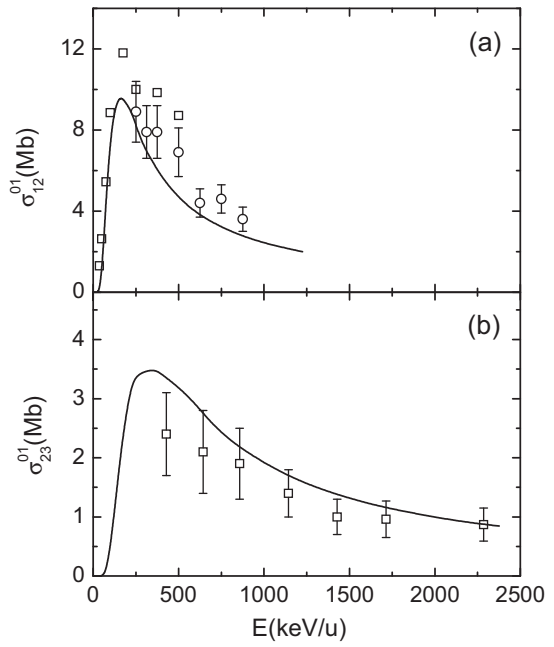

Fig. 5. Cross sections (in Mb) for electron loss accompanied by single ionization in collisions of ions with helium as a function of the projectile energy. Calculation: solid line. (a) $He^+ + He$. Experiment: open squares, Ref. [10]; open circles, Ref. [14]. (b) $Li^{2+} + He$. Experiment: open squares, Ref. [13].

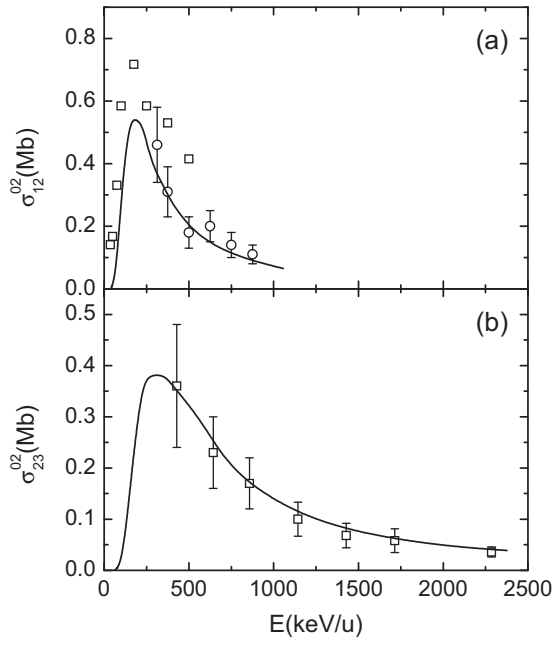

Fig. 6. Cross sections (in Mb) for electron loss accompanied by double ionization in collisions of ions with helium as a function of the projectile energy. Calculation: solid line. (a) He^+ + He. Experiment: open squares, Ref. [10]; open circles, Ref. [14]. (b) Li^{2+} + He. Experiment: open squares, Ref. [13].

The above equation can be further written as

$$\frac{d}{d\nu_P}\left[\frac{\sqrt{q_T}}{\tau'}\left(\frac{\sqrt{r'}/\nu'_e}{\nu_P}-\frac{2\sqrt{q_T}}{\nu_P^3}\right)\right]=0 \tag{23}$$

The extremum condition

$$E_{\max}=\frac{1}{2}\nu_P^2=3\nu'_e\sqrt{q_T/r'}, \tag{24}$$

For one-electron ions

$$\nu'_e\propto 1/\sqrt{r'}\quad I'\propto 1/r', \tag{25}$$

where I' is the ionization energy of the projectile electron. Thus

$$E_{\max}\propto I'\sqrt{q_T}, \tag{26}$$

which indicates that the peak position for electron loss will move towards the higher energy with the increasing q_T and I'. Obviously, I' for Li^{2+} is larger than that for He^+. On the other hand, as discussed above, due to the larger effective charge q_P for Li^{2+}, the actual effective charge q_T in collision with Li^{2+} should be larger than that with He^+. It also suggests that, for the given projectile and process, the value of E_{max} for the He target should be larger than that for the H target, which is consistent with the experimental data and the present calculations.

For the electron loss associated with the target ionization, except for the factor discussed above, the target ionization should be considered. In the same way, the ionization probability $F_I(\rho'=0)$ will reach a maximum when

$$\frac{dF_I(\rho=0)}{d\nu_P}=0, \tag{27}$$

We have

$$E_{\max}\propto I\sqrt{q_P} \tag{28}$$

where I is the ionization energy of the target electron. This is expected to be helpful for understanding the results. In addition, it should be emphasized that both q_T and q_P are closely related to the projectile nucleus charge Z_P.

For the given process, target, it is also obvious from the results that the cross sections by Li^{2+} is smaller than that by He^+. This can be understood from Eqs. (22) to (25). The electron-loss probability at $\rho'=0$, $E=E_{\max}$ is

$$F_L(\rho'=0)\big|_{E_{\max}}\propto q_T^{1/4}r'^{3/4}\nu'^{-1/2}_e\propto\frac{q_T^{1/4}}{I'}. \tag{29}$$

Due to the increase of the projectile nucleus charge, a larger q_T is induced. However, at the same time, the projectile electron distributes closer to the nucleus, i.e., the average distance r' decreases, which gives rise to the larger binding energy. According to the analysis through Eq. (29), the smaller cross section by Li^{2+} should be attributed to the stronger binding energy that the electron of Li^{2+} ions suffers from the projectile nucleus. As far as the target for a certain process, the cross sections for He are larger than those for H. This is by the reason of two factors. On the one hand, the larger q_T for He contributes to the larger cross section. On the other hand, the capture probability is suppressed to some extent because of the larger binding energy of the electron for He.

For a given projectile, the cross section maximum ratio of single electron loss with ionization to single electron loss is approximately in proportion to the ionization probability. Similarly with Eq. (29), the ionization probability at $\rho=0$, $E=E_{\max}$ is

$$F_I(\rho=0)\big|_{E_{\max}}\propto q_P^{1/4}/I \tag{30}$$

That is, the ionization probability decreases with the increasing ionization energy I and the decreasing effective charge q_P. Because the ionization energy for H is larger than the first ionization energy for He, for a given projectile, the cross section maximum ratio relations satisfy that $\sigma_{12}^{01}/\sigma_{12}(\mathrm{He})>\sigma_{12}^{01}/\sigma_{12}(\mathrm{H})$, $\sigma_{23}^{01}/\sigma_{23}(\mathrm{He})>\sigma_{23}^{01}/\sigma_{23}(\mathrm{H})$. On the other hand, for a given target, It is can be seen that the cross section maximum ratios $\sigma_{12}^{01}/\sigma_{12}(\mathrm{H})<\sigma_{23}^{01}/\sigma_{23}(\mathrm{H})$, $\sigma_{12}^{01}/\sigma_{12}(\mathrm{He})<\sigma_{23}^{01}/\sigma_{23}(\mathrm{He})$, $\sigma_{12}^{02}/\sigma_{12}(\mathrm{He})<\sigma_{23}^{02}/\sigma_{23}(\mathrm{He})$. This is because the q_P value for Li^{2+} is larger than that for He^+.

4. Conclusions

In conclusion, we have extended our works to evaluate the cross sections for single electron loss (SL), single electron loss associated with single ionization (SLSI) and single electron loss associated with double ionization (SLDI) in collisions of one-electron ions He^+, Li^{2+} with atomic hydrogen and helium in low- and intermediate-energy regime. The calculated results are compared with the available experimental data. It is found that our results present a general good agreement with the experiments. For a given impact energy and process, the range of the effective impact parameter is related to electron distributions and effective charges of both collision partners. At the same time the results show that such range for the SL, SLSI and SLDI decrease in sequence. Due to the stronger binding energy from which the electron of Li^{2+} suffers, for the given process and target, the cross section induced by Li^{2+} is smaller than that by He^+. On the other hand, for the certain process and projectile, the cross section for the He target is larger than that for the H target, which is attributed to the larger effective charge and the binding energy for He. The present calculations can predict the peak position correctly. The peak position moves towards the higher energy with the effective charges and the binding energy of the projectile and the target. At the same time, the relationships between the maximum value ratios for cross sections can understood through the differences of the target ionization energy and the effective projectile charge.

Acknowledgements

Supports from the National Natural Science Foundation (NSF) of China Grant No. 10704030, the Fundamental Research Funds for the Central Universities Grant No. lzujbky-2010-26 and the Natural Science Foundation (NSF) of Gansu province Grant Nos. 1107RJZA096 and 0710RJZA014 are gratefully acknowledged.

References

[1] A.K. Kaminskii, A.A. Vasilev, Phys. Part. Nucl. 29 (1998) 201.
[2] W.H. Liu, D.R. Schultz, Astrophys. J. 530 (2000) 500.
[3] J.S. Yoon, Y.D. Jung, Phys. Plasmas 6 (1999) 3391.
[4] R.D. DuBois, et al., Phys. Rev. A 70 (2004) 032712.
[5] T.R. Dillingham, J.R. Macdonald, P. Richard, Phys. Rev. A 24 (1981) 1237.
[6] M.B. Shah, T.V. Goffe, H.B. Gilbody, J. Phys. B Atom. Mol. Phys. 10 (1977) L723.
[7] M.M. Sant'Anna, W.S. Melo, A.C.F. Santos, G.M. Sigaud, E.C. Montenegro, Phys. Rev. A 58 (1998) 1204.
[8] P. Hvelplund, A. Andersen, Phys. Scr. 26 (1982) 370.
[9] M.B. Shah, H.B. Gilbody, J. Phys. B: At. Mol. Opt. Phys. 24 (1991) 977.
[10] R.D. DuBois, Phys. Rev. A 39 (1989) 4440.
[11] M.M. Sant'Anna, W.S. Melo, A.C.F. Santos, G.M. Sigaud, E.C. Montenegro, Nucl. Instrum. Methods Phys. Res. B 99 (1995) 46.
[12] H. Knudsen, L.H. Andersen, H.K. Haugen, P. Hvelplund, Phys. Scr. 26 (1982) 132.
[13] O. Woitke, P.A. Závodszky, S.M. Ferguson, J.H. Houck, J.A. Tanis, Phys. Rev. A 57 (1998) 2692.
[14] A.C.F. Santos1, G.M. Sigaud, W.S. Melo, M.M. Sant'Anna, E.C. Montenegro, J. Phys. B: At. Mol. Opt. Phys. 44 (2011) 045202.
[15] J. Fiol, R.E. Olson, A.C.F. Santos, G.M. Sigaud, E.C. Montenegro, J. Phys. B: At. Mol. Opt. Phys. 34 (2001) L503.
[16] J.A. Tanis, E.M. Bernstein, M.W. Clark, S.M. Ferguson, R.N. Price, Phys. Rev. A 43 (1991) 4723.
[17] Amal K. Saha, L.C. Tribedi, K.V. Thulasi Ram, K.G. Prasad, P.N. Padon, Phys. Scr. T80 (1999) 384.
[18] N. Bohr, L. Lindhard, K. Dan Vidensk, Selsk. Mat. Fys. Medd. 28 (1954) 7.
[19] D. Brandt, Nucl. Instr. Method B 214 (1983) 93.
[20] I. Ben-Itzhak, A. Jain, O.L. Weaver, J. Phys. B Atom. Mol. Opt. Phys. 26 (1993) 1711.
[21] B.W. Ding, B.H. Wang, B.T. Hu, Phys. Lett. A 373 (2009) 3047.
[22] B.W. Ding, D.Y. Yu, Int. J. Mass. Spectrom. 299 (2011) 59.
[23] B.W. Ding, X.M. Chen, D.Y. Yu, H.B. Fu, G.Z. Sun, Y.W. Liu, Phys. Rev. A 78 (2008) 062718.
[24] B.W. Ding, X.M. Chen, D.Y. Yu, B.T. Hu, X.H. Cai, Z.Y. Liu, Int. J. Mass. Spectrom. 285 (2009) 157.
[25] V.A. Sidorovich, V.S. Nikolaev, Phys. Rev. A 31 (1985) 2193.